Published in final edited form as:

Arthritis Rheumatol. 2016 May ; 68(5): 1251–1261. doi:10.1002/art.39575.

Netrin-1 regulates fibrocyte accumulation in the decellularized fibrotic scleroderma lung microenvironment and in bleomycin induced pulmonary fibrosis

Huanxing Sun[1,*], **Yangyang Zhu**[1,*], **Hongyi Pan**[1,*], **Xiaosong Chen**[1], **Jenna L. Balestrini**[2], **TuKiet T. Lam**[3], **Jean E. Kanyo**[3], **Anne Eichmann**[4], **Mridu Gulati**[1], **Wassim H. Fares**[1], **Hanwen Bai**[5], **Carol A. Feghali-Bostwick**[6], **Ye Gan**[1], **Xueyan Peng**[1], **Meagan W. Moore**[1], **Eric S. White**[7], **Parid Sava**[8], **Anjelica L. Gonzalez**[8], **Yuwei Cheng**[9], **Laura E. Niklason**[2], and **Erica L. Herzog**[1]

[1]Department of Internal Medicine, Section of Pulmonary, Critical Care, and Sleep Medicine, Yale University School of Medicine, New Haven, CT, 06520

[2]Department of Anesthesiology, Yale School of Medicine, New Haven, CT, 06520

[3]Department of Molecular Biophysics and Biochemistry, Yale School of Medicine, New Haven, CT, 06520

[4]Cardiovascular Institute, Yale School of Medicine, New Haven, CT, 06520

[5]Department of Genetics, Yale School of Medicine, New Haven, CT, 06520

[6]Department of Medicine, Medical University of South Carolina, Charleston, SC

[7]Department of Internal Medicine, University of Michigan, Ann Arbor, Michigan

[8]Yale School of Engineering, New Haven, CT, 06520

[9]Program of Computational Biology and Bioinformatics, Yale University, New Haven CT 06520

Abstract

Objectives—Fibrocytes are collagen-producing leukocytes that accumulate in Scleroderma-associated interstitial lung disease (SSc-ILD) via unknown mechanisms. The extracellular matrix (ECM) influences cellular phenotypes. However, a relationship between the lung ECM and fibrocytes in Scleroderma has not been explored. This study uses a novel translational platform based on decellularized human lungs to determine whether the scleroderma lung ECM controls fibrocyte development from peripheral blood mononuclear cells.

Methods—Decellularized scaffolds prepared from healthy and fibrotic Scleroderma lung explants underwent biomechanical evaluation using tensile testing and biochemical analysis using proteomics. Cells from healthy and SSc-ILD subjects were cultured on these scaffolds, and CD45+Pro-ColIα1+ cells meeting criteria for fibrocytes were quantified. The contribution of

Address for Correspondence: Erica L. Herzog, MD, PhD, 300 Cedar Street, TAC 441S, New Haven CT 06520-8057, Phone 203 785 3627, Fax 203 785 3826, erica.herzog@yale.edu.

*These authors contributed equally to this work.

Netrin-1 to fibrosis was assessed using neutralizing antibodies in this system and via the inhalational administration of bleomycin to Netrin-1+/− mice.

Results—Compared to control lung scaffold, SSc-ILD lung scaffolds showed aberrant anatomy, enhanced stiffness, and abnormal extracellular matrix composition. Culture of control cells in Scleroderma scaffolds increased Pro-ColIα1+ production, which was stimulated by enhanced stiffness and abnormal ECM composition. SSc-ILD cells demonstrated increased Pro-ColIα1 responsiveness to Scleroderma lung scaffolds, but not enhanced stiffness. Enhanced Netrin-1 expression was seen on $CD14^{lo}$ SSc-ILD cells and antibody mediated Netrin-1 neutralization attenuated CD45+Pro-ColIα1+ detection in all settings. Netrin-1+/− mice were protected from bleomycin induced lung fibrosis and fibrocyte accumulation.

Conclusion—Factors present in Scleroderma lung matrices regulate fibrocyte accumulation via a Netrin-1-dependent pathway. Netrin-1 regulates bleomycin induced murine pulmonary fibrosis. Netrin-1 might be a novel therapeutic target in SSc-ILD.

Introduction

Scleroderma (Systemic Sclerosis, SSc) is an idiopathic autoimmune disease characterized by cutaneous and visceral fibrosis (1) in which many patients are affected by interstitial lung disease (SSc-ILD) which lacks specific, highly efficacious therapy (2). The response of SSc-ILD to immunomodulation and in some cases bone marrow transplantation suggests involvement of leukocytes in disease pathogenesis (2). Lung tissue obtained from patients with SSc-ILD frequently contains inflammatory cells juxtaposed with extracellular matrix (ECM) (2). To date, however, there exists scant information regarding how inflammatory cell phenotypes might be influenced by the SSc-ILD ECM. When viewed in this light it is notable that fibrocytes, a population of leukocytes possessing mesenchymal characteristics that are associated with multiple inflammatory conditions (3, 4), demonstrate enhanced accumulation in the blood and/or lungs of patients with SSc-ILD (5–7). However, the significance of these cells and the factors regulating their appearance in this clinical context remains unknown.

The ECM supports organ structure and essential cellular processes (8). Bioengineering-based strategies have emerged as useful tools to study cell-matrix interactions in several contexts (9–11). Cells grown in decellularized matrices produced from healthy and diseased lungs recapitulate mesenchymal and epithelial features of diseases such as Idiopathic Pulmonary Fibrosis (IPF) (12, 13) and Chronic Obstructive Pulmonary Disease (COPD) (14) through processes involving biochemical and/or mechanical interactions. Because these studies have focused on ECM interactions with cells of presumed pulmonary origin, the effect of the mammalian lung matrisome on recruited immune cells is unknown and the ECM's ability to control fibrosis-promoting properties in cells of bone marrow origin has not been fully evaluated in autoimmune diseases such as SSc-ILD. It is therefore relevant that functional abnormalities are detected in immune cells exposed to ECM fragments (15) and that mechanotransductive signaling modulates innate and adaptive immune responses (16). However the contribution of these factors to development of circulating mesenchymal cells such as fibrocytes in the setting of human lung fibrosis in general, and SSc-ILD in particular, has not been defined.

Netrin-1 belongs to a family of evolutionarily conserved laminin-like secreted proteins that interact with attractive or repulsive receptors to control axon guidance in developing nerves. These processes may involve direct interactions with the ECM as well as mechanotransductive responses (17–19). Netrins are also expressed outside the nervous system where they regulate branching, morphogenesis and angiogenesis [reviewed in (20, 21)]. Netrin-1-expressing human leukocytes have been reported (22) and differential expression of several Netrin-1 receptors both predicts reduced event free survival in Idiopathic Pulmonary Fibrosis (23) and controls the development of experimentally induced lung fibrosis in mice (24). However, while Netrin-1 regulates the activation and migration of monocyte-derived cells (25, 26), an effect on fibrocyte biology in the context of SSc-ILD remains unexplored.

We evaluated whether the human lung ECM regulates the appearance of collagen producing, fibrocyte-like cells in cultured human PBMCs. We characterized the anatomic, biochemical, and mechanical properties of a three dimensional model of the fibrotic lung microenvironment created from decellularized human normal and SSc-ILD lung explants, assessed whether these parameters regulate spontaneous collagen production by healthy and SSc-ILD PBMCs, and defined the contribution of Netrin-1 to these processes in both the decellularized human lung and in the bleomycin model of murine lung fibrosis.

MATERIALS AND METHODS

Detailed experimental methods exist in the online supplement.

Subject recruitment

For the leukocyte work, Studies were performed with institutional approval and explicit informed consent. Subjects age >21 with a diagnosis of SSc-ILD were eligible. Exclusion criteria included inability to provide informed consent, pregnancy, malignancy, active smoking, and primary airway process. Demographically matched normal controls were recruited from the greater New Haven Community (6).

Blood drawing and processing

30 to 50 ml of peripheral blood was drawn into heparinized tubes and peripheral blood mononuclear cells (PBMCs) were isolated using Ficoll separation (Stem Cell Technologies) as previously described (6).

Preparation of human lung scaffold slices

Explanted human lung tissue obtained from the University of Pittsburgh or University of Michigan lung transplant programs, or the Yale Rapid Autopsy Program, was decellularized via modifications of previously published work (11, 27–29). Acellularity was assessed via histologic, biochemical, and scanning electron microscopy methods (27) as detailed in the online supplement.

Histologic analysis

Samples were stained with hematoxylin and eosin, Masson's Trichrome, Verhoeff Van and Gieson (VVG) to assess gross morphology, collagen fibers and elastin fibers (30).

Tensile testing

Decellularized lungs were analyzed using an Instron 5848 as described in the online supplement.

Sample preparation and mass spectrometry

Sample preparation and Mass Spectrometry was performed on an LTQ-Orbitrap ELITE LC MS/MS mass spectrometer equipped with a Waters nanoACQUITY™ UPLC™ system in the Yale School of Medicine as published in the online supplement.

Seeding of lung scaffolds with PBMCs

Prepared slices were placed in a Poly-L-Lysine coated 6-well plate (Becton Dickinson, Two Oak Park, Bedford, MA), seeded with 1×10^6 PBMCs. Medium was partially changed after 24 hours and then every 48 hours thereafter for a maximum culture period of 14 days. Full details can be found in the supplement.

Immunofluorescence

Immunofluorescence is described in the online supplement.

Polyacrylamide hydrogel preparation and usage

Polyacrylamide hydrogels were prepared as previously described (31). Briefly, amino-silanated coverslips were treated with 0.1M NaOH and 3-Aminopropyltriethoxysilane (Sigma-Aldrich, St Louis, MO) while chloro-silanated coverslips were treated with dichlorodimethylsilane (Sigma-Aldrich, St Louis, MO). Polyacrylamide solutions of varying stiffness were prepared by altering the concentrations of acrylamide (Bio-Rad Laboratories Inc, Hercules, CA) and bis-acrylamide (Bio-Rad Laboratories Inc, Hercules, CA), cross linked with direct UV light (365 nm, 10 mW/cm^2). Gels were coated with human plasma fibronectin (EMD Millipore, Billerica, MA), and Young's Modulus (measure of elasticity) of gels was assessed using a modified model of the Hertz equation using a custom made apparatus as described (31). Gels were sterilized, rinsed and placed into ultra-low attachment surface polystyrene 6-well-plates (Corning Incorporated, Corning, NY). 3×10^6 PBMCs suspended in 2 ml medium were drizzled over the gel and cultured in serum-containing conditions for fourteen days.

Extracellular matrix solution preparation

Decellularized lung scaffolds were lyophilized, lysed, and dialyzed. Final protein concentration was analyzed using the Bio-Rad protein assay dye reagent concentrate Kit (Bio-Rad Laboratories Inc, Hercules, CA) in a Beckman Coulter DU 530 (Beckman Institute, Urbana, IL).

PBMCs treated with ECM solutions

1×10^6 PBMCs in 950μl medium were seeded into 12-well-plates and ECM solution was added for a final concentration of 1 μg/ml. Medium was changed every 48 hours and cells were harvested after fourteen days.

Antibody-mediated Netrin blockade

1×10^6 PBMCs were seeded on lung scaffold slices and cultured for fourteen days in the presence of 10μg/ml anti-Netrin-1 neutralizing antibody or IgG control (R&D Systems, Minneapolis, MN) added to the medium at the time of cell seeding and in all subsequent media changes.

Scanning electron microscopy (SEM)

SEM was performed as described more fully in the online supplement.

Quantitative reverse transcriptase PCR

Total cellular RNA was isolated from PBMCs using Trizol as described (4). Quantitative RT-PCR was performed using predesigned and validated primers against human Netrin-1 or β-actin. Relative expression was determined using the 2^{deltaCt} method.

Flow Cytometry

Cells were processed for flow cytometry and analyzed using a FACS Calibur as previously described (32). Data were analyzed using Flowjo (TreeStar Inc, Ashland, OR).

Animal studies

Animal studies were performed with approval from Yale's Institutional Animal Care and Use Committee (IACUC). Because Netrin-1−/− mice are embryonic lethal, Netrin-1 heterozygote null mice were used for this study (33). Mice were backcrossed onto the C57/BL6 background for at least ten generations and wild type littermates were used as controls.

Bleomycin administration

Sex-matched, 8-week-old wild-type, NTN+/− mice (n≥4 per group) received a single orotracheal bleomycin inhalation (2.5 U/kg; Hospira Pharmaceuticals). Mice were sacrificed and evaluated at day 14 as described (28).

Sacrifice and tissue harvest

Terminal anaesthesia, bronchoalveolar lavage, median sternotomy, right heart perfusion, and *en bloc* heart and lung removal was achieved as described (34).

Quantification of lung collagen

Collagen content was determined by quantifying total soluble collagen using the Sircol Collagen Assay kit (Biocolor, Accurate Chemical and Scientific Corp.) according to the manufacturer's instructions (35).

Modified Ashcroft Scores

Lung fibrosis was quantified histologically using the modified Ashcroft grading system (36).

Flow Cytometry of mouse lung tissue

Resected lung tissue was minced, digested in dispase, and analyzed for CD45 and ColIα1 expression via flow cytometry as previously reported (35).

Statistics

Statistical comparison of continuous data was performed using paired or unpaired Student's t-test, Mann Whitney U test, or ANOVA with Bonferroni post-test as appropriate. Statistical management of the proteomics data is described in the online supplement. A p value of <0.05 following correction for multiple comparisons was considered significant.

RESULTS

Decellularized fibrotic scleroderma lungs display abnormal anatomy and structure

In order to develop an *in vitro* three-dimensional model of the fibrotic lung microenvironment, we utilized decellularized matrix from healthy and diseased lungs. "Healthy" tissues were obtained from explanted normal lungs declined for use in orthotopic lung transplantation (n=3, Figure 1A). Fibrotic lung tissue was obtained from SSc-ILD lung explants removed at the time of transplantation (n=7, Figure 1A). Tissues were decellularized using a modified procedure based on previously published work (28, 29, 37). Decellularization was confirmed by cellular absence on DAPI staining (Figure 1A), by the >99% removal of DNA quantified fluorometrically (Figure 1B) and by negative immunoblotting for GAPDH (Figure 1B). Structural assessment by H&E staining and SEM revealed that, relative to control lung scaffold (CLS), SSc-ILD lung scaffold (SLS) exhibited disrupted tissue architecture characterized by replacement of alveolar spaces with conglomerate ECM (Figure 1C). These data show that decellularized scaffolds prepared from SSc-ILD explants display anatomic abnormalities at the macro, micro, and ultrastructural level.

Decellularized fibrotic scleroderma lungs show an abnormal matrix composition

Given the excessive ECM visualized in the SSc-ILD lung scaffolds, we next evaluated the biochemical composition of control and SSc-ILD matrices (n=3 each). Here, CLS (n=3) and SLS (n=3) underwent proteomic analysis utilizing a bottom-up Label-free LCMS Quantitation technique with protein identification False Discovery Rate of <1% with quantitation calculation based on normalization to the total protein abundance in each sample. This analysis revealed alterations in glycoproteins, collagens, and proteoglycans (Table 1, Figure S1, and Table S1) in the SLS, several of which were confirmed by histochemistry on paraffin embedded sections (Figure S1). Some of these changes, such as Periostin, are similar to those previously reported for decellularized IPF lungs (11) though other changes such as Fibulin 3, TINAG-like 1, and Elastin appear more specific to SSc-ILD. These data indicate a unique composition of proteoglycans, glycoproteins, and collagens comprises the SLS.

Decellularized fibrotic scleroderma lung scaffolds demonstrate abnormal compliance

We also evaluated the mechanical properties of CLS (n=2) and SLS (n=5) lung scaffolds using Instron-based tensile testing. Here, at the low deformation range (the physiological levels of strain during breathing) comparison of tensile testing revealed a 6.14-fold increase in Young's modulus in SLS relative to CLS ($p=0.0023$, Figure 1D). While such changes would be expected in the setting of fibrosis (11), to our knowledge ours are the first data to quantify this property in SSc-ILD, thereby framing altered mechanical conditions as a potential contributory factor to this disease.

Scleroderma lung scaffolds demonstrate enhanced support of Pro-Collα1 production by human PBMCs

Having defined the anatomic, biochemical, and mechanical properties of the CLS and SLS, we next evaluated whether these characteristics differentially regulate collagen expression by cultured human leukocytes. Here, freshly isolated PBMCs obtained from control subjects (n=4) were seeded into CLS and SLS and cultured for up to 14 days in serum-containing conditions. Scaffolds were harvested, fixed, and assessed for the presence of collagen-producing leukocytes based on co-expression of CD45 and Pro-ColIα1. CD45+Pro-ColIα1+ cells displaying different morphologies were seen, including small cells with little cytoplasm, large rounded cells with abundant cytoplasm, and spindle-shape cells with an elongated aspect ratio (Fig. S2). Because the significance of these morphologic changes is unclear at this time, all fibrocyte-like CD45+Pro-ColIα1+ cells were included in the results. Additional analysis revealed abundant expression of fibronectin by these cell populations (Fig. S3) and absent expression of αSMA (Fig. S3), supporting prior work indicating that while recruited leukocytes can adopt an ECM expression phenotype, without additional stimulation they are unlikely to serve as a dominant source of myofibroblasts. When quantification of these fibrocytes or fibrocyte-like cells was performed, only a small percentage of CD45+ cells grown in the CLS co-expressed Pro-ColIα1, a finding that was increased by 2.85-fold in the SLS ($p<0.0054$, Figure 2A). These data indicate that the low grade support of PBMC-derived Pro-ColIα1 expression by normal human lung scaffolds is enhanced in scaffolds prepared from SSc-ILD lungs.

Normal human PBMCs stimulated with SSc-ILD lung ECM display increased expression of Pro-Collα1

Having determined that factors present in SSc-ILD ECM microenvironment influence expression of Pro-ColIα1 by normal PBMCs, we explored whether these findings stem from biochemical interactions. Freshly isolated control PBMCs were grown under serum-containing conditions for fourteen days in the presence of medium supplemented with digested CLS or SLS at a concentration of 1 ug/ml which in pilot studies had been determined the optimal dose for these studies (data not shown). Here we found that the low level detection of CD45+ Pro-ColIα1+ cells seen in the CLS-exposed cells was increased by 1.89-fold fold in the presence of SLS ($p<0.04$, n=5, Fig 2B). More detailed studies in which leukocytes were stimulated with microfibril associated protein-4 (MFAP4), the most highly detected protein in the SLS, revealed that to this glycoprotein is sufficient to increase detection of Pro-ColIα1+ in leukocytes obtained from normal controls (Fig. S4). These data

indicate that the digestible components of the decellularized SSc-ILD lung, particularly MFAP4, are sufficient to stimulate collagen production in normal human PBMCs.

Normal human PBMCs cultured on stiff hydrogels display increased expression of Pro-Col Iα1

Direct contact with stiff surfaces regulate mesenchymal properties and functions of fibroblasts (38, 39) however to date such an effect has not been demonstrated in leukocytes. We addressed this question by culturing freshly isolated healthy PBMCs on tunable hydrogels constructed with the approximate stiffness seen in the normal (4 kPa) and fibrotic (20 kPa) human lung scaffolds shown in Figure 1. Here, low level detection of CD45+Pro-ColIα1+ cells was seen in the samples grown on the 4kPa gels, which was increased by more than 3.27-fold in the cells grown on the 20 kPa gels ($p<0.04$, n=3, Figure 2C). These studies show that in addition to direct interactions with components of the diseased matrix, cellular responses to local substrate stiffness also contribute to the enhanced expression of Pro-ColIα1 by PBMCs cultured in the SLS.

SSc-ILD demonstrate increased Pro-Colα1 responses to decellularized scaffolds and digested SLS, but not stiff hydrogels

These data suggested that local factors substantially regulate the collagen-producing phenotype of leukocytes that come into contact with the lung ECM. In order to determine whether intrinsic cellular properties might also be involved, experiments were performed using PBMCs obtained from subjects with SSc-ILD, which have been previously reported to contain increased fibrocytes compared to healthy controls (5–7). Here, SSc-ILD PBMCs were noted to engender low proportions of CD45+Pro-ColIα1+ in the CLS that were significantly enhanced in the SLS ($p=0.0011$, Figure 3A). Similar to controls, SSc-ILD PBMCs demonstrated abundant fibronectin and absent α-SMA (Figure S5) and scanning electron microscopy revealed both rounded and spindle shaped cells (Fig. S5). The response of SSc-ILD PBMCs to the SLS was 3.54-fold greater than that of controls ($p=0.043$, Fig. 3A). Interestingly, relative to control cells, SSc-ILD PBMCs displayed a 3.15-fold more robust response to stimulation with digested SLS ($p=0.0033$, Fig. 3B) and a 41% increase in fibrocytes resulting from stimulation with MFAP4 ($p=0.03$, Fig. S5 and S6). In addition, SSc-ILD PBMCs responded to stiff hydrogels with 3.63-fold increased collagen production relative to soft hydrogels ($p=0.043$, Fig. 3C) but the overall magnitude of this response did not differ from that of control PBMCs ($p=0.45$, Fig.3C). When viewed in combination, these data indicate that SSc-ILD PBMCs display augmented Pro-ColIα1 expression when cultured on SLS and that the difference in the magnitude of this response may be dominated by protein components of the SLS such as MFAP4.

Increased Netrin-1 expression by SSc-ILD CD14^{lo} monocytes

The data presented above indicate the ability of human PBMCs to adopt a collagen-producing phenotype in response to the biochemical properties of SSc-ILD lung ECM is enhanced in the SSc-ILD disease state. Because the digested SLS displays a markedly different protein composition than CLS, we explored cellular factors that might regulate interactions with the ECM in health and disease. Here we were led to evaluate a role for Netrin-1, a laminin-like protein that regulates cell: matrix interactions in the developing

nervous system (19) that has been recently associated with disease outcome in IPF but to date remains unexplored in the context of systemic fibrosing diseases such as scleroderma. Because differential detection of Netrin-1 was not found in comparison of the CLS vs. SLS, we reasoned that any effect of this protein on fibrocyte development must result from autocrine or paracrine expression by leukocytes. In order to explore this issue, we first assessed expression of Netrin-1 gene, NTN-1, in archived control (n=30) and SSc-ILD (n=20) PBMCs and found 3.12-fold higher NTN-1 expression relative to β-actin in the setting of SSc-ILD (p=0.019, Fig. S7). Prospective evaluation of Netrin-1 expression using FACS revealed that Netrin-1 to be expressed on circulating monocytes where 4.01-fold increased detection of $CD14^{lo}$NTN-1+ monocytes was seen in the subjects with SSc-ILD (n=5) relative to control (n=4, p=0.006, Fig. 4A). In contrast, the proportion of $CD14^{hi}$NTN-1+ monocytes was unchanged between SSc-ILD and control (Fig. S7). These data show that the increased detection of Netrin-1 in SSc-ILD is due in part to augmented expression on a subset of $CD14^{lo}$ monocytes.

Netrin-1 neutralization attenuates collagen production by PBMCs cultured in decellularized lung scaffolds

The finding of increased NTN-1 expression in SSc-ILD suggested that this protein might be involved in the regulation of collagen production by leukocytes. To evaluate the validity of this hypothesis, immunodetection of Netrin-1 was performed on control and SSc-ILD PBMCs cultured in the CLS and SLS. Here, quite interestingly, Netrin-1 detection was close to absent in the cells grown in the CLS whereas it was expressed quite robustly in both the control and Ssc-ILD PBMCs cultured in the SLS (Fig. S8), suggesting that it might mediate the fibrocyte accumulation seen in this setting. In order to explore this concept, PBMCs obtained from control (n=3) or SSc-ILD subjects (n=5) were obtained and cultured in CLS or SLS for fourteen days in the presence or absence of Netrin-1 neutralizing antibody. Here, Netrin-1 neutralization reduced detection of CD45+Pro-ColIα1+ cells in all settings with the largest reduction found in the SSc-ILD PBMCs cultured in the SLS. ($p<0.05$ all comparisons, Fig. 5B and 5C). These data show that Netrin-1 controls expression of Pro-ColIα1 by leukocytes that come into contact with decellularized lung tissue, and that this effect is greatest in the setting of SSc-ILD.

Netrin-1 deficiency attenuates bleomycin-induced lung fibrosis and fibrocyte accumulation in mice

Last, in order to determine whether Netrin-1 participates in fibrosis and fibrocyte accumulation *in vivo*, mice that were heterozygote deficient for the Netrin-1 locus (NTN-1+/−) were administered a single inhaled dose of bleomycin, sacrificed after fourteen days and evaluated for the effect of Netrin-1 partial deficiency on fibrosis-relevant endpoints including lung inflammation, fibrosis, and CD45+ColIα1+ cells (n≥4 mice/group). Here, while there was no effect of Netrin-1 deficiency on BAL cell counts (Fig. 5A), we did detect a 34.8% reduction in total soluble collagen content ($p<0.038$, Fig. 5A, B) that was accompanied by a 41.6% reduction in the histologic appearance of fibrosis based on modified Ashcroft scores (Fig. 5B) and a 47.9% reduction in CD45+ColIα1+ cells meeting flow cytometric criteria for fibrocytes (p=0.033 Fig. 5C). These data indicate that Netrin-1

mediates collagen accumulation along with the appearance of CD45+ColIα1+ cells in the fibrotic mammalian lung.

DISCUSSION

These studies use a novel translational platform to demonstrate that the accumulation of collagen-producing leukocytes is regulated by biochemical and mechanical aspects of the human lung ECM, and that SSc-ILD PBMCs display increased responsiveness to the digestible components of the decellularized fibrotic Scleroderma lung. Furthermore, Netrin-1 expression is increased on $CD14^{lo}$ monocytes from subjects with SSc-ILD where it regulates leukocyte-matrix interactions in the decellularized lung. Last, studies performed in the bleomycin model of pulmonary fibrosis demonstrate that partial deficiency of Netrin-1 ameliorates histologic and biochemical determinants of fibrosis, and the accumulation of CD45+ColIα1+ cells, indicating that neutralization of NTN-1 might serve as a novel therapeutic target in this context. These studies have many ramifications for SSc-ILD and, potentially, for inflammatory and fibrotic diseases affecting the lung, liver, kidney, and skin.

Since their discovery in 1994 (40), fibrocytes remain a focus of investigation in the area of fibrosis and tissue remodeling (4). The current study advances the field to demonstrate that the appearance of fibrocytes or fibrocyte-like cells is regulated both by the biochemical components of the ECM as well as by local responses to enhanced tissue stiffness. These data not only support a recent study showing that exposure to fibrotic lung matrix induces transcriptional expression of ECM proteins in primary lung fibroblasts (41), but also demonstrate that ECM proteins such as the glycoprotein MFAP4 can induce similar events in cells of hematopoietic origin. Whether this represents an intermediate event in altered cell fate specification from leukocyte to fibroblast will require additional study, as will elucidation of the specific biochemical factors accounting for these observations. We were somewhat surprised to find that while SSc-ILD PBMCs appeared primed to respond to the tensile properties and matrix composition of the SLS, overall quantities of CD45+Pro-ColIα1+ cells did not differ between control and SSc-ILD samples in any context. This finding may be due to the small sample size, to the range of stiffness employed in the hydrogel studies, to inhibition of Netrin-1 and/or Collagen expression by the healthy lung scaffold, or alterations in Netrin-1 receptor expression, and raises the possibility that additional factors such as trafficking, transmigration, adhesion, and survival might also determine the quantities of CD45+Pro-ColIα1+ cells present in any given tissue. Interactions with additional resident stromal populations might be important as well, as shown by one recent study in which normal lung fibroblasts could inhibit fibrocyte differentiation via the regulated secretion of the Netrin-1-related protein Slit2 (42). Synthesis of these data suggest a paradigm in which contact with diseased ECM and loss of suppressive fibroblast properties permit the enhanced accumulation of CD45+Pro-Colα1+ cells that have been reported in the in SSc-ILD lung (5, 7).

It is increasingly recognized that cellular responses to local tissue stiffness regulate cellular phenotypes (43, 44). In the context of pulmonary fibrosis, this process is best defined in tissue-resident fibroblasts (13). While studies performed in normal cells have evaluated mechanotransductive regulation of adaptive lymphocyte responses (45), to our knowledge

ours are the first studies implicating mechanotransductive responses in the regulation of collagen production by leukocytes. Given the systemic and visceral fibrosis characterizing the scleroderma disease state, our findings may extend beyond the lung to carry more global ramifications for scleroderma in general. It is also likely that additional dynamic factors influence leukocyte biology such as alterations in laminar flow, responses to local stiffness during capillary transmigration, and durotaxis across diseased tissue might be relevant. Development of improved experimental methodologies incorporating salient properties of flow and migration will be critical factors in this area.

Since its discovery several decades ago, Netrin-1 and its receptors have been shown to critically regulate axonal guidance (18) and vascular development (33). Recent studies indicate that Netrin-1-expressing monocytes/macrophages regulate inflammation and pathologic remodeling in the lung (22), adipose tissue (46), and blood vessels (47). Our data extends this body of work by demonstrating a previously unrecognized association of Netrin-1 with Scleroderma where it mediates the enhanced propensity of SSc-ILD leukocytes to adopt collagen production in a three dimensional model of the fibrotic SSc-ILD microenvironment and in a murine model of pulmonary fibrosis. While we have not determined the receptor(s) through which Netrin-1 enacts these effects, it is possible that Unc5 homologues [which predict reduced event free survival when overexpressed in PBMCs in the setting of Idiopathic Pulmonary Fibrosis (23)] or ADORA2B [which has been recently revealed as a central regulator of experimentally induced lung fibrosis in mice (24)], may be involved. Further work is required to evaluate these questions. Because we have also found Netrin-1 deficiency reduced detection of fibrosis and CD45+ColIα1+ cells in the bleomycin model, our data also suggest that Netrin-1 based therapeutics might be efficacious in SSc-ILD. However, because Netrin-1 is known to be expressed on a number of cells, further work will be required to ascertain the mechanism through which Netrin-1 deficiency is fibroprotective.

Given the novel nature of our studies, many additional questions remain. The cell population(s) capable of adopting collagen expression in this context have not been defined, though previous studies suggest that CD14+ monocytes are at least partially involved (40). The nature of the analytical method used for proteomic evaluation may be difficult to apply to the intact fibrotic lung, though at least several of the results in our studies appear valid based on immunofluorescence and/or bioactivity. Comparison of the tensile properties of the native and decellularized lung will be important in future experiments, as the scaffolds in our study displayed tensile properties approximating the upper end of what has been reported for the normal mammalian lung (39). The relative effects of Netrin-1 neutralization on cell:matrix interactions and mechanosensing remain to be defined, as do the receptors and signaling pathways though which Netrin-1 regulates collagen production by human leukocytes and experimentally induced lung fibrosis. We have not determined how the NTN-1-expressing, $CD14^{lo}$ cells seen in SSc-ILD are related to the enhanced responsiveness of SSc-ILD PBMCs to the SLS. Last, we have not determined whether these findings extend to Scleroderma patients without ILD, a question that will require the development of decellularized skin matrices. Nevertheless, our work firmly establishes biochemical and mechanical biologic cues, and Netrin-1, as new areas of investigation in the

immunopathogenesis of fibrosis. Development of additional platforms and *in vivo* lineage tracing systems will allow further exploration of these areas in the field of SSc-ILD.

Supplementary Material

Refer to Web version on PubMed Central for supplementary material.

Acknowledgments

We thank Xin Du and Lin Leng for helpful suggestions and technical assistance. We also acknowledge Mary LoPresti and Kathrin Wilczak for their assistance with the proteomics sample preparation and analysis of the Label-free quantitation, respectively.

Funding: National Institutes of Health grant numbers HL109033, CTSA SpiRIT award, AR061271, NIH-SIG-RR031795 for MS instrument, U01 HL111016, UL1 RR024153, UL1TR000005, P30 AR061271, K24 AR060297.

REFERENCES CITED

1. Gabrielli A, Avvedimento EV, Krieg T. Scleroderma. The New England journal of medicine. 2009; 360(19):1989–2003. [PubMed: 19420368]
2. Herzog EL, Mathur A, Tager AM, Feghali-Bostwick C, Schneider F, Varga J. Interstitial lung disease associated with systemic sclerosis and idiopathic pulmonary fibrosis: How similar and distinct? Arthritis & rheumatology. 2014
3. Galligan CL, Fish EN. The role of circulating fibrocytes in inflammation and autoimmunity. Journal of leukocyte biology. 2013; 93(1):45–50. [PubMed: 22993208]
4. Reilkoff RA, Bucala R, Herzog EL. Fibrocytes: emerging effector cells in chronic inflammation. Nature reviews Immunology. 2011; 11(6):427–35.
5. Borie R, Quesnel C, Phin S, Debray MP, Marchal-Somme J, Tiev K, et al. Detection of alveolar fibrocytes in idiopathic pulmonary fibrosis and systemic sclerosis. PloS one. 2013; 8(1):e53736. [PubMed: 23341987]
6. Mathai SK, Gulati M, Peng X, Russell TR, Shaw AC, Rubinowitz AN, et al. Circulating monocytes from systemic sclerosis patients with interstitial lung disease show an enhanced profibrotic phenotype. Laboratory Investigation. 2010; 90(6):812–23. [PubMed: 20404807]
7. Tourkina E, Bonner M, Oates J, Hofbauer A, Richard M, Znoyko S, et al. Altered monocyte and fibrocyte phenotype and function in scleroderma interstitial lung disease: reversal by caveolin-1 scaffolding domain peptide. Fibrogenesis & tissue repair. 2011; 4(1):1–13. [PubMed: 21211003]
8. Hynes RO, Naba A. Overview of the matrisome–an inventory of extracellular matrix constituents and functions. Cold Spring Harbor perspectives in biology. 2012; 4(1):a004903. [PubMed: 21937732]
9. Petersen TH, Calle EA, Zhao L, Lee EJ, Gui L, Raredon MB, et al. Tissue-engineered lungs for in vivo implantation. Science. 2010; 329(5991):538–41. [PubMed: 20576850]
10. Cortiella J, Niles J, Cantu A, Brettler A, Pham A, Vargas G, et al. Influence of acellular natural lung matrix on murine embryonic stem cell differentiation and tissue formation. Tissue Engineering Part A. 2010; 16(8):2565–80. [PubMed: 20408765]
11. Booth AJ, Hadley R, Cornett AM, Dreffs AA, Matthes SA, Tsui JL, et al. Acellular normal and fibrotic human lung matrices as a culture system for in vitro investigation. American journal of respiratory and critical care medicine. 2012; 186(9):866–76. [PubMed: 22936357]
12. Parker MW, Rossi D, Peterson M, Smith K, Sikstrom K, White ES, et al. Fibrotic extracellular matrix activates a profibrotic positive feedback loop. The Journal of clinical investigation. 2014; 124(4):1622–35. [PubMed: 24590289]
13. Booth AJ, Hadley R, Cornett AM, Dreffs AA, Matthes SA, Tsui JL, et al. Acellular normal and fibrotic human lung matrices as a culture system for in vitro investigation. Am J Respir Crit Care Med. 2012; 186(9):866–76. [PubMed: 22936357]

14. Wagner DE, Bonenfant NR, Parsons CS, Sokocevic D, Brooks EM, Borg ZD, et al. Comparative decellularization and recellularization of normal versus emphysematous human lungs. Biomaterials. 2014; 35(10):3281–97. [PubMed: 24461327]
15. Sorokin L. The impact of the extracellular matrix on inflammation. Nature reviews Immunology. 2010; 10(10):712–23.
16. Jaalouk DE, Lammerding J. Mechanotransduction gone awry. Nature reviews Molecular cell biology. 2009; 10(1):63–73. [PubMed: 19197333]
17. Moore SW, Zhang X, Lynch CD, Sheetz MP. Netrin-1 attracts axons through FAK-dependent mechanotransduction. The Journal of neuroscience: the official journal of the Society for Neuroscience. 2012; 32(34):11574–85. [PubMed: 22915102]
18. Duman-Scheel M. Netrin and DCC: axon guidance regulators at the intersection of nervous system development and cancer. Current drug targets. 2009; 10(7):602–10. [PubMed: 19601764]
19. Yebra M, Montgomery AM, Diaferia GR, Kaido T, Silletti S, Perez B, et al. Recognition of the neural chemoattractant Netrin-1 by integrins alpha6beta4 and alpha3beta1 regulates epithelial cell adhesion and migration. Developmental cell. 2003; 5(5):695–707. [PubMed: 14602071]
20. Rajasekharan S, Kennedy TE. The netrin protein family. Genome Biol. 2009; 10(9):239. [PubMed: 19785719]
21. Cirulli V, Yebra M. Netrins: beyond the brain. Nat Rev Mol Cell Biol. 2007; 8(4):296–306. [PubMed: 17356579]
22. Mirakaj V, Dalli J, Granja T, Rosenberger P, Serhan CN. Vagus nerve controls resolution and pro-resolving mediators of inflammation. The Journal of experimental medicine. 2014; 211(6):1037–48. [PubMed: 24863066]
23. Herazo-Maya JD, Noth I, Duncan SR, Kim S, Ma SF, Tseng GC, et al. Peripheral blood mononuclear cell gene expression profiles predict poor outcome in idiopathic pulmonary fibrosis. Science translational medicine. 2013; 5(205):205ra136.
24. Karmouty-Quintana H, Philip K, Acero LF, Chen NY, Weng T, Molina JG, et al. Deletion of ADORA2B from myeloid cells dampens lung fibrosis and pulmonary hypertension. FASEB journal: official publication of the Federation of American Societies for Experimental Biology. 2015; 29(1):50–60. [PubMed: 25318478]
25. Tadagavadi RK, Wang W, Ramesh G. Netrin-1 regulates Th1/Th2/Th17 cytokine production and inflammation through UNC5B receptor and protects kidney against ischemia-reperfusion injury. J Immunol. 185(6):3750–8.
26. Wang W, Reeves WB, Pays L, Mehlen P, Ramesh G. Netrin-1 overexpression protects kidney from ischemia reperfusion injury by suppressing apoptosis. Am J Pathol. 2009; 175(3):1010–8. [PubMed: 19700747]
27. Sun H, Calle E, Chen X, Mathur A, Zhu Y, Mendez J, et al. Fibroblast engraftment in the decellularized mouse lung occurs via a β1-integrin-dependent, FAK-dependent pathway that is mediated by ERK and opposed by AKT. American Journal of Physiology-Lung Cellular and Molecular Physiology. 2014; 306(6):L463–L75. [PubMed: 24337923]
28. Zhou Y, Peng H, Sun H, Peng X, Tang C, Gan Y, et al. Chitinase 3-like 1 suppresses injury and promotes fibroproliferative responses in Mammalian lung fibrosis. Science translational medicine. 2014; 6(240):240ra76.
29. Petersen TH, Calle EA, Zhao L, Lee EJ, Gui L, Raredon MB, et al. Tissue-engineered lungs for in vivo implantation. Science. 2010; 329(5991):538–41. [PubMed: 20576850]
30. Thomas H, Petersen EAC, Zhao Liping, Lee Eun Jung, Gui Liqiong, Raredon MichaSam B, Gavilov Kseniya, Yi Tai, Zhuang Zhen W, Breuer Christopher, Herzog Erica, Niklason Laura E. Tissue-Engineered Lungs for in Vivo Implantation. Science. 2010; 329:4.
31. Tse, JR., Engler, AJ. Preparation of hydrogel substrates with tunable mechanical properties. Current protocols in cell biology. Bonifacino, Juan S., et al., editors. 2010. Chapter 10: Unit 10 6
32. Mathai SK, Gulati M, Peng X, Russell TR, Shaw AC, Rubinowitz AN, et al. Circulating monocytes from systemic sclerosis patients with interstitial lung disease show an enhanced profibrotic phenotype. Laboratory investigation; a journal of technical methods and pathology. 2010; 90(6):812–23. [PubMed: 20404807]

33. Lu X, Le Noble F, Yuan L, Jiang Q, De Lafarge B, Sugiyama D, et al. The netrin receptor UNC5B mediates guidance events controlling morphogenesis of the vascular system. Nature. 2004; 432(7014):179–86. [PubMed: 15510105]
34. Lee CG, Cho SJ, Kang MJ, Chapoval SP, Lee PJ, Noble PW, et al. Early growth response gene 1–mediated apoptosis is essential for transforming growth factor β1–induced pulmonary fibrosis. The Journal of experimental medicine. 2004; 200(3):377–89. [PubMed: 15289506]
35. Gan Y, Reilkoff R, Peng X, Russell T, Chen Q, Mathai SK, et al. Role of semaphorin 7a signaling in transforming growth factor beta1-induced lung fibrosis and scleroderma-related interstitial lung disease. Arthritis and rheumatism. 2011; 63(8):2484–94. [PubMed: 21484765]
36. Hubner RH, Gitter W, El Mokhtari NE, Mathiak M, Both M, Bolte H, et al. Standardized quantification of pulmonary fibrosis in histological samples. BioTechniques. 2008; 44(4):507–11. 14–7. [PubMed: 18476815]
37. Sun H, Calle E, Chen X, Mathur A, Zhu Y, Mendez J, et al. Fibroblast engraftment in the decellularized mouse lung occurs via a beta1-integrin-dependent, FAK-dependent pathway that is mediated by ERK and opposed by AKT. American journal of physiology Lung cellular and molecular physiology. 2014; 306(6):L463–75. [PubMed: 24337923]
38. Hecker L, Logsdon NJ, Kurundkar D, Kurundkar A, Bernard K, Hock T, et al. Reversal of persistent fibrosis in aging by targeting Nox4-Nrf2 redox imbalance. Science translational medicine. 2014; 6(231):231ra47.
39. Liu F, Mih JD, Shea BS, Kho AT, Sharif AS, Tager AM, et al. Feedback amplification of fibrosis through matrix stiffening and COX-2 suppression. The Journal of cell biology. 2010; 190(4):693–706. [PubMed: 20733059]
40. Bucala R, Spiegel L, Chesney J, Hogan M, Cerami A. Circulating fibrocytes define a new leukocyte subpopulation that mediates tissue repair. Molecular medicine. 1994; 1(1):71. [PubMed: 8790603]
41. Bitterman PB, Wewers MD, Rennard SI, Adelberg S, Crystal RG. Modulation of alveolar macrophage-driven fibroblast proliferation by alternative macrophage mediators. The Journal of clinical investigation. 1986; 77(3):700–8. [PubMed: 3081573]
42. Pilling D, Zheng Z, Vakil V, Gomer RH. Fibroblasts secrete Slit2 to inhibit fibrocyte differentiation and fibrosis. Proceedings of the National Academy of Sciences of the United States of America. 2014; 111(51):18291–6. [PubMed: 25489114]
43. Humphrey JD, Dufresne ER, Schwartz MA. Mechanotransduction and extracellular matrix homeostasis. Nature reviews Molecular cell biology. 2014; 15(12):802–12. [PubMed: 25355505]
44. Balestrini JL, Chaudhry S, Sarrazy V, Koehler A, Hinz B. The mechanical memory of lung myofibroblasts. Integrative biology: quantitative biosciences from nano to macro. 2012; 4(4):410–21. [PubMed: 22410748]
45. Wang JH, Reinherz EL. The structural basis of alphabeta T-lineage immune recognition: TCR docking topologies, mechanotransduction, and co-receptor function. Immunological reviews. 2012; 250(1):102–19. [PubMed: 23046125]
46. Ramkhelawon B, Hennessy EJ, Menager M, Ray TD, Sheedy FJ, Hutchison S, et al. Netrin-1 promotes adipose tissue macrophage retention and insulin resistance in obesity. Nature medicine. 2014; 20(4):377–84.
47. Ramkhelawon B, Yang Y, van Gils JM, Hewing B, Rayner KJ, Parathath S, et al. Hypoxia induces netrin-1 and Unc5b in atherosclerotic plaques: mechanism for macrophage retention and survival. Arteriosclerosis, thrombosis, and vascular biology. 2013; 33(6):1180–8.

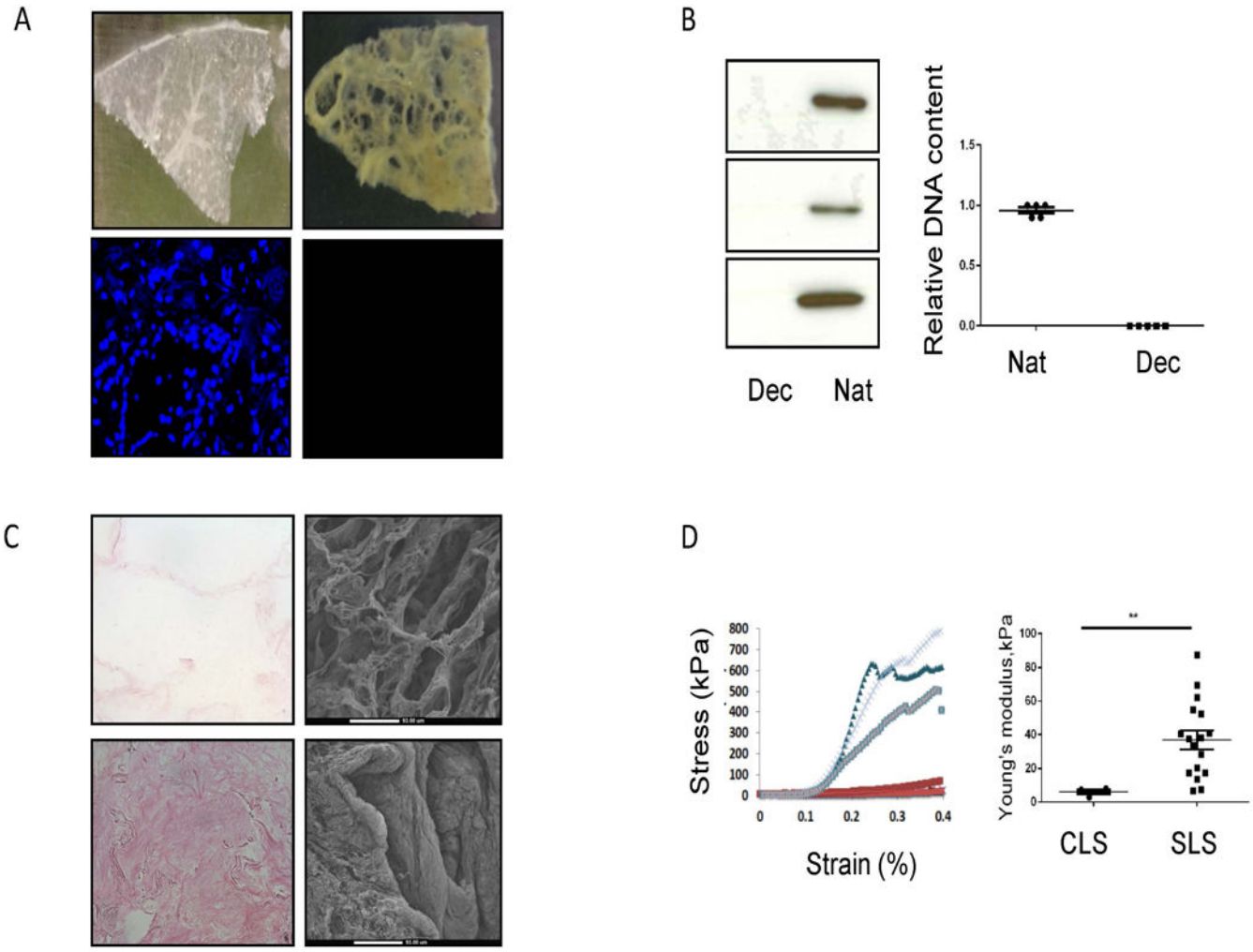

Figure 1.

A. Top: gross appearance of control (left) and SSc-ILD (right) scaffolds. Bottom: DAPI staining of native and decellularized SSc-ILD lung. B. Left: Western Blot for GAPDH on native ("Nat," n=3) and decellularized ("Dec." n=3) SSc-ILD lungs. Right: fluorometic detection of DNA in native vs. decellularized lung. C. Comparison of H&E staining (left) and SEM (right) on CLS (top) and SLS (bottom). D. Left: comparison of Young's modulus in scaffolds prepared from control (red) and SSc-ILD (blue). Right: Relative to control (n=2), Young's modulus (kPa) is increased at the low deformation range in SLS (n=5). **P<0.01. Dec: kPa = kilopascals. Data are shown as mean +/− SEM.

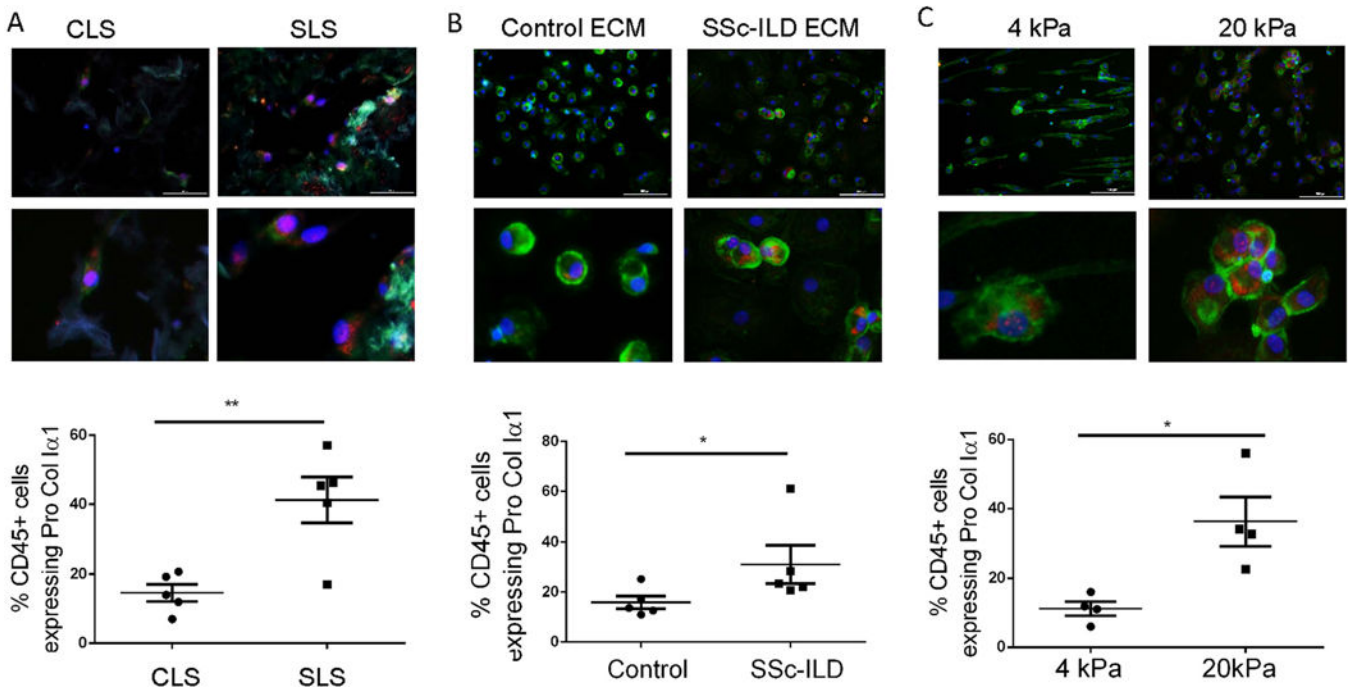

Figure 2.

A. Top: Low and high power view of Pro-ColIα1 (red) and CD45 (green) immunostaining of control PBMCs in CLS and SLS. Bottom: Comparison of CD45+Pro-ColIα1+ cells of control PBMCs in CLS and SLS. B. Top: Low and high power view of Pro-ColIα1 and CD45 double staining of control PBMCs treated with digested CLS and SLS. Bottom: Comparison of CD45+Pro-ColIα1+ cells of control PBMCs treated with digested CLS and SLS. C. Top: Low and high power view of Pro-ColIα1 and CD45 immunostaining of control PBMCs grown on 4 kPa and 20 kPa Polyacrylamide Hydrogel. Bottom: comparison of CD45+Pro-ColIα1+ cells in control PBMCs grown on 4 kPa and 20 kPa Polyacrylamide Hydrogel. *P<0.05, **P<0.01. In all images CD45 is in the green FITC channel, Pro-ColIα1+ is in the Texas Red channel, and nuclei are counterstained with DAPI. Scale bar =100 microns. Data are shown as mean +/− SEM.

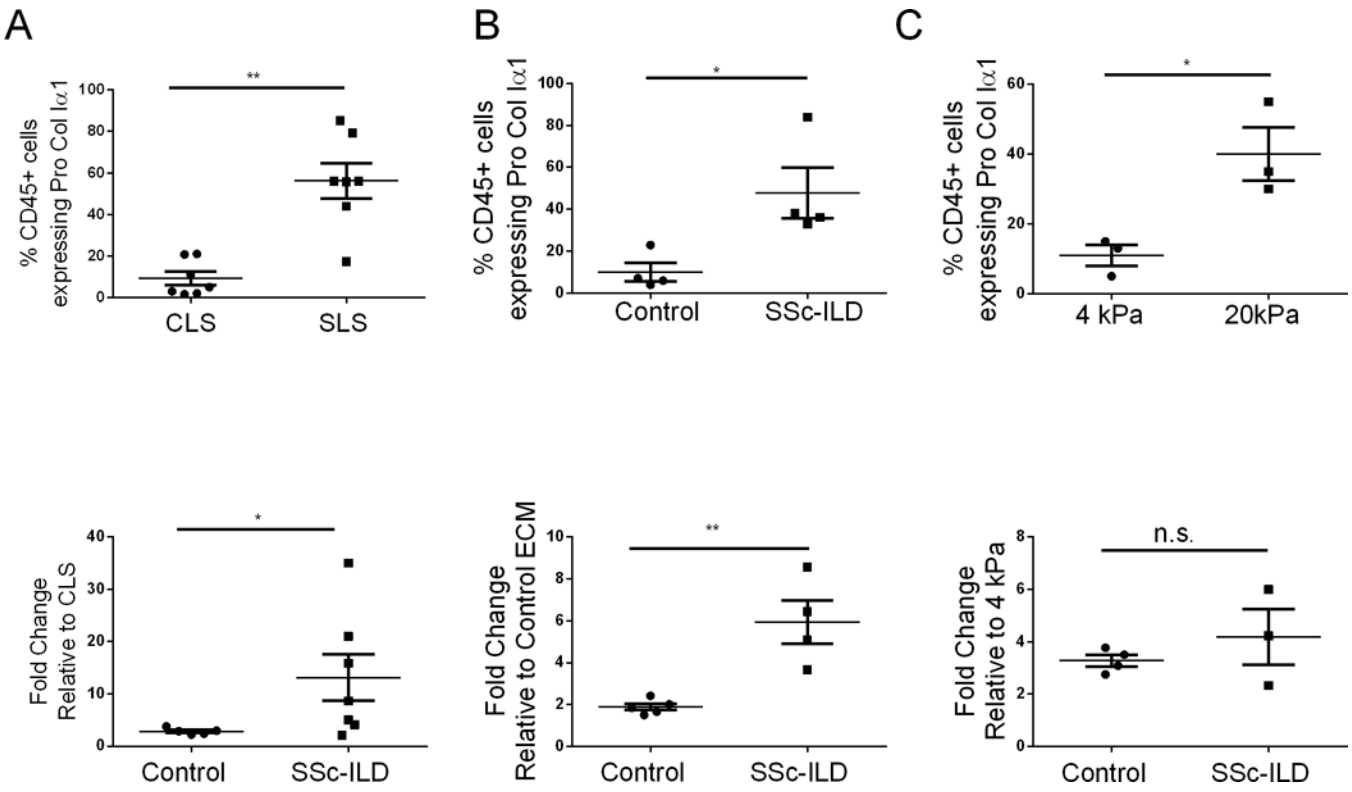

Figure 3.

A. Top: Percentage of CD45+Pro-ColIα1+ cells of SSc-ILD PBMCs grown in CLS and SLS. Bottom: comparison of the fold-increase to SLS in CD45+Pro-ColIα1+ cells between control and SSc-ILD PBMCs. B. Top: Percentage of CD45+Pro-ColIα1+ cells in SSC-ILD PBMCs treated with control and SSc-ILD digested ECM. Bottom: comparison of the fold-increase in CD45+Pro-ColIα1+ cells between control and SSc-ILD PBMCs grown in control vs SSc-ILD digested ECM. C. Top: Percentage of CD45+Pro-ColIα1+ cells in SSC-ILD PBMCs grown on 4 kPa vs 20 kPa Polyacrylamide Hydrogel. Bottom: comparison of the fold-increase in CD45+Pro-ColIα1+ cells between control and SSc-ILD PBMCs grown on 4 kPa vs 20 kPa Polyacrylamide Hydrogel. *P<0.05, **P<0.001. n.s. = not significant. Data are shown as mean +/− SEM.

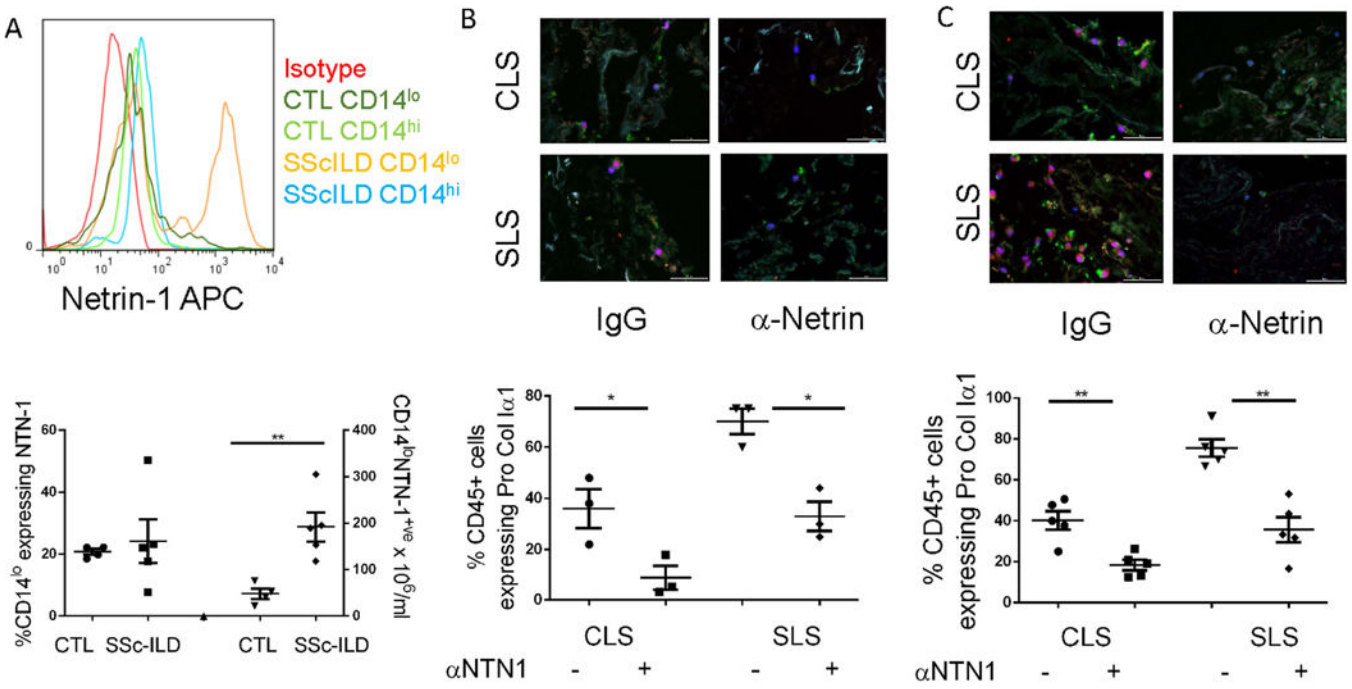

Figure 4.

A. Top: Histogram displaying expression of Netrin-1 (NTN-1) on populations of $CD14^{lo}$ or $CD14^{hi}$ monocytes in control vs. SSc-ILD. Bottom: relative to control (CTL), concentrations (right axis) but not percentages (left axis) of $CD14^{lo}$ monocytes co-expressing Netrin-1 are significantly elevated in SSc-ILD PBMCs. B. Effect of antibody mediated Netrin-1 blockade on percentages of CD45+Pro-ColIα1+ cells when healthy PBMCs are grown in CLS and SLS in the presence of either IgG or Netrin-1 neutralizing antibody (α-Netrin). C. Effect of antibody mediated Netrin-1 blockade on percentages of CD45+Pro-ColIα1+ cells when SSc-ILD PBMCs are grown in CLS and SLS in the presence of either IgG or Netrin-1 neutralizing antibody (α-Netrin). *P<0.05, **P<0.01. Data are shown as mean +/− SEM.

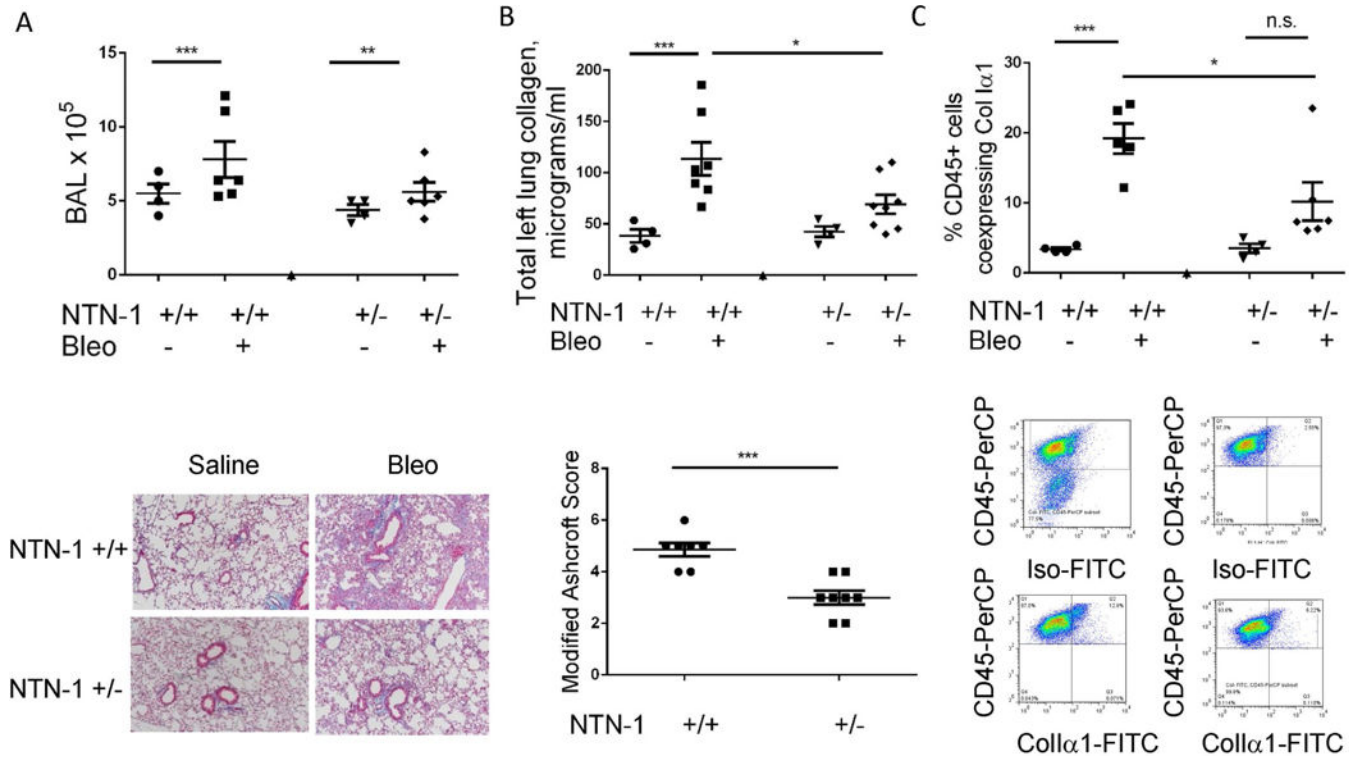

Figure 5.

A. Top: Quantification of BAL inflammation in saline and bleomycin (Bleo) treated Netrin$^{+/+}$ (wild type) and Netrin$^{+/-}$ mice. Bottom: Trichrome staining of lung tissue from saline and bleomycin (Bleo)-treated Netrin$^{+/+}$ and Netrin$^{+/-}$ mice. B. Top: Lung collagen content measured by Sircol analysis. Bottom: Modified Ashcroft scores in bleomycin-treated Netrin$^{+/+}$ and Netrin$^{+/-}$ mice. C. Top: Relative to wild type mice, percentages of CD45+cells co-expressing ColIα1+ are reduced in bleomycin-treated Netrin-1$^{+/-}$mice. Bottom: FACS-based detection of CD45+ ColIα1+ cells. Cells are stained with CD45 and isotype control to select the CD45+ population (upper left panel). The negative gate for the FITC channel is established (upper right) and applied to bleomycin-challenged WT mice (lower left) and NTN+/− mice (lower right). CD45+ cells obtained from Bleomycin challenged NTN+/− mice display a smaller percentage of ColIα1+ cells. *P<0.05, **P<0.01. ***P<0.001. Data are shown as mean +/− SEM.

Table 1

Relative detection of matrisome proteins (* fold change in SLS relative to CLS)

Protein	*SLS/CLS	Protein	*SLS/CLS
MFAP4	3.86	Neutrophil elastase	0.46
Periostin	2.97	Collagen alpha-4(IV) chain	0.49
Dermatopontin	2.34	Agrin	0.51
EMILIN-1	2.25	Bone marrow proteoglycan	0.56
Heparan Sulfate Proteoglycan	2.22	Collagen alpha-1(XXI) chain	0.58
Fibrillin-1	2.06	WISP-2	0.7
Fibulin-5	1.91	Metalloproteinase inhibitor 3	0.71
Fibulin 3	1.88	Collagen alpha-3(V) chain	0.73
Elastin	1.8	Prolargin	0.73
TINAG-like 1	1.71	Biglycan	0.77
Laminin subunit alpha-4	1.68	Laminin subunit gamma-1	0.8
Fibulin-1	1.65	Vitronectin	0.8
Fibulin-2	1.52	Collagen alpha-6(VI) chain	0.82
Collagen alpha-1(IV) chain	1.51	Laminin subunit alpha-5	0.84
Lumican	1.47	Laminin subunit beta-2	0.84
Collagen alpha-2(VIII) chain	1.44	Nephronectin	0.85